Biosensors and Bioelectronics 51 (2014) 336–342

Contents lists available at ScienceDirect

Biosensors and Bioelectronics

journal homepage: www.elsevier.com/locate/bios

Inhibition of G-quadruplex assembling by DNA ligation: A versatile and non-covalent labeling strategy for bioanalysis

Jiangtao Ren [a,b], Jiahai Wang [a], Jin Wang [a,c,*], Erkang Wang [a,*]

[a] State Key Laboratory of Electroanalytical Chemistry, Changchun Institute of Applied Chemistry, Chinese Academy of Sciences, Changchun, Jilin 130022, China

[b] University of Chinese Academy of Sciences, Beijing 100049, China

[c] Department of Chemistry and Department of Physics, State University of New York at Stony Brook, NY 11794, USA

ARTICLE INFO

Article history:
Received 15 April 2013
Received in revised form
27 July 2013
Accepted 30 July 2013
Available online 6 August 2013

Keywords:
G-quadruplex
DNA ligation
Fluorescent probe
Non-covalent labeling

ABSTRACT

Through tuning relative thermodynamic stabilities (I, II and III), DNA ligation was coupled to split G-quadruplex probes and a versatile, non-covalent labelling and fluorescent strategy was constructed based on inhibition of template-directed G-quadruplex assembling by ligation reaction. The non-covalent complex between G-quadruplex and fluorescent probe was employed as signalling label and thus covalent modification of DNA probes with fluorescent probes was avoided. Selective detection of small biomolecules (ATP and NAD^+) in the nanomolar range was realized due to the cofactor-dependent activity of DNA ligases (T4 and *Escherichia coli* DNA ligase). By virtue of the simple strategy, the effect of mismatch position of single-base mismatched template DNA on the ligation efficiency was validated. Meanwhile, highly mismatch-influenced ligation efficiency of ligase endows the cost-effective strategy great potential for single-nucleotide polymorphism (SNP) analysis. The non-covalent labeling strategy provides a versatile and cost-effective platform for monitor of DNA ligation, cofactor detection, SNP analysis and other ligase-based assays.

1. Introduction

Functional nucleic acids (FNAs), such as aptamer, DNAzyme and so on, have been well developed and utilized for constructing varieties of novel sensing systems (Liu et al., 2009). Nucleic acid enzymes (NAEs) (e.g. polymerase, nuclease) have been widely coupled to nucleic acid technology for bioanalysis (Hu and Zhang, 2010; Jia et al., 2010; Song et al., 2012a; Zuo et al., 2010). Some enzymatic reactions require the presence of specific biomolecule (cofactor), which can provide a novel platform for highly selective detection of these cofactors (Ma et al., 2008). Based on the sequence-specific activity, NAEs were also utilized for analysis of single-nucleotide polymorphisms (SNPs) (Xiao et al., 2012). In this study, we combined G-quadruplex FNA with NAEs together and fabricated one non-covalent labeling and versatile platform for selective biomolecule detection.

Adenosine triphosphate (ATP) often called as "molecular unit of energy currency", is essential and critical for all organisms (Gourine et al., 2005), and its depletion induces some diseases, such as hypoxia, hypoglycemia and ischemia (Harkness and Saugstad, 1997). Numerous biosensors have been constructed for ATP detection based on organic molecules (Xu et al., 2009; Zyryanov et al., 2007), especially DNA aptamer (Guo et al., 2011; Lu et al., 2010; Sitaula et al., 2012; Song et al., 2012b; Tang et al., 2008). However, most of them cannot effectively discriminate ATP from its analogues, such as adenosine (A), adenosine monophosphate (AMP) and adenosine diphosphate (ADP). Nicotinamide adenine dinucleotide (NAD^+) as another important biomolecule in all life forms, plays a significant role in transcriptional regulation, calorie restriction mediated lifespan extension, and age-associated diseases (Lin and Guarente, 2003). Analogous to ATP, the traditional approach of enzymatic cycling assay for NAD^+ is unable to discriminate NAD^+ from reduced nicotinamide adenine dinucleotide (NADH) and other analogues (Lowry et al., 1961). Alternative techniques have been developed, including HPLC, ESI-MS/MS and NMR etc, and expensive equipment and complex procedures were inevitable (Yamada et al., 2006). Recently, a few fluorescent and electrochemical biosensors were constructed for sensing ATP and NAD^+, based on the cofactor-dependent DNA ligation (Lu et al., 2011; Tang et al., 2011; Wang et al., 2010; Zhao et al., 2012), which totally resolved the selectivity problem. SNPs are the most abundant class of genetic variations in the human genome and SNP analysis is significant for the early diagnosis and treatment of the disease (Savas and Liu, 2009). Due to exceptional discrimination ability to single-base mismatched sequences, DNA ligases have been applied for genotyping and DNA sequencing (Conze et al., 2009). In recent year, some ligase-based

* Corresponding authors. Tel.: +86 431 8526 2003; fax: +86 431 8568 9711.
E-mail addresses: jin.wang.1@stonybrook.edu (J. Wang), ekwang@ciac.jl.cn (E. Wang).

0956-5663/$ - see front matter © 2013 Published by Elsevier B.V.
http://dx.doi.org/10.1016/j.bios.2013.07.059

assays furnished effective strategies, e.g. nanoparticle-coupled DNA ligation, and realized highly sensitive and selective nucleic acid detection and multiplex SNP typing (Wee et al., 2012; Xue et al., 2009).

However, most of previous sensing systems for cofactor detection and SNP analysis required covalent modification of the DNA probes with different tags (e.g. fluorescent dyes and biotin) to convert molecular recognition events to detectable signals, such as fluorescence (Jhaveri et al., 2000; Song et al., 2012b), color (Wang et al., 2007; Xue et al., 2009) and electrochemical signal (Ma et al., 2008; Wee et al., 2012), resulting in extra cost, complexity and limitation for practical application.

G-quadruplex DNA as one kind of significant FNAs, has been paid significant attention due to its versatility and stimulus-responsive reconfiguration (Burge et al., 2006). Lots of "label-free" biosensors were constructed based on the non-covalent complexes, which exhibited the peroxidase-mimicking activity from G-quadruplex-hemin complex (Li et al., 2009, 2010b), or fluorescence enhancement from G-quadruplex-specific fluorescent probes (Li et al., 2010a; Zhang et al., 2012). Since the template DNA-directed reassembly of split G-quadruplex was first utilized for visualizing single nucleotide polymorphisms (Kolpashchikov, 2008), the non-covalent labeling strategy has been developed and systematically investigated for colorimetric and fluorescent analysis of DNA (Nakayama and Sintim, 2009; Ren et al., 2011, 2012). Herein, by coupling DNA ligation to split G-quadruplex probes and based on the cofactor-dependent and mismatch-influenced ligation efficiency of DNA ligase, we constructed two non-covalent labeling biosensors for selective detection of cofactors (ATP and NAD^+), investigated the ligation efficiency of ligases using single-base mismatched template DNA and provided a potential cost-effective method for SNP screening.

As shown in Scheme 1, DNA ligase can catalyze the ligation of two captured probes (Ca and Cb) hybridized to adjacent position of perfectly matched template DNA (PM). By hybridization in the complementary segments, the template PM promotes the split G-quadruplex probes (P1/P2) to assemble into G-quadruplex which is able to bind G-quadruplex-specific fluorescent probes (*N*-methyl mesoporphyrin IX, NMM) and induces fluorescence enhancement (Ren et al., 2012). Ascribe to the distinction of the thermodynamic stabilities (duplex II > the G-quadruplex-duplex hybrid structure III > the nicked duplex I), the DNA ligation and duplex II production inhibit assembling of split G-quadruplex, and trigger the fluorescence decrease from the non-covalent G-quadruplex-NMM complex. Based on the cofactor-dependent and sequence-dependent ligation efficiency of DNA ligase, the resulting fluorescence changes provide a versatile and non-covalent labeling platform for simple and selective detection of cofactors (ATP and NAD^+) and discrimination of single base differences in the template DNA.

2. Materials and methods

2.1. Materials

Ultrapage-purified oligonucleotides (Tables S1 and S2), adenosine triphosphate (ATP), cytidine triphosphate (CTP), guanosine triphosphate (GTP), uridine triphosphate (UTP) and tris(hydroxymethyl)aminomethane (Tris) were obtained from Sangon Biotechnology Co., Ltd (Shanghai, China). Adenosine (A), adenosine monophosphate (AMP) and adenosine diphosphate (ADP) were obtained from Sigma-Aldrich (USA). Nicotinamide adenine dinucleotide (NAD^+), the reduced form of nicotinamide adenine dinucleotide (NADH), nicotinamide adenine dinucleotide phosphate (NADP), and nicotinamide adenine dinucleotide phosphate hydride (NADPH) were purchased from Gen-View Scientific Inc. (USA). T4 DNA ligase (350 U/μL) and *Escherichia coli (E. coli)* DNA ligase (60 U/μL) were from TaKaRa Biotechnology Co., Ltd (Dalian, China). *N*-methyl mesoporphyrin IX (NMM) was purchased from Frontier Scientific, Inc. (Logan, Utah, USA). T4 buffer solution (pH = 7.6) containing 660 mM Tris, 66 mM $MgCl_2$ and 100 mM dithiothreitol was used for ligation reaction of T4 DNA ligase. E buffer (pH = 8.0) containing 300 mM Tris, 40 mM $MgCl_2$, 100 mM $(NH_4)_2SO_4$, and 12 mM EDTA, and BSA (0.05%) were used for ligation reaction of *E. coli* DNA ligase. The Tris–HAc buffer (25 mM Tris, pH = 7.4) was used for sample preparation throughout.

2.2. Sequence design and optimization

The split G-quadruplex probes (P1/P2) were obtained by splitting the c-Myc G-qudruplex DNA (TGAGGG TGGGGAGGGTGGG-GAA) into two asymmetric fragments flanked with the sequences that were complementary to the template PM. Four groups of complementary DNAs of perfectly matched template (PM) were utilized (Ca1/Cb1 and C1, Ca2/Cb2 and C2, Ca3/Cb3 and C3, Ca4/Cb4 and C4) for sequence optimization. These complementary DNAs had different sequence lengths. C DNAs were corresponding to the ligation products of DNA ligation of the two short chains

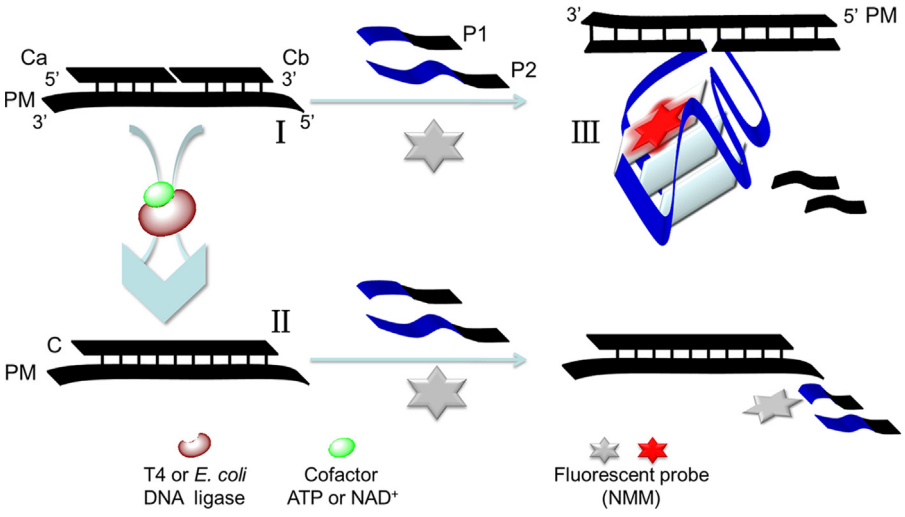

Scheme 1. Inhibition of split G-quadruplex assembling by DNA ligation for cofactor detection and SNP discrimination of PM based on the cofactor-dependent and mismatch-influenced ligation efficiency of DNA ligase.

(Ca/Cb). In Tris-HAc buffer, PM (8 μL, 10 μM) and KCl (20 μL, 1 M) were mixed and reacted with each group of Ca (8 μL, 10 μM) and Cb (8 μL, 10 μM), or C (8 μL, 10 μM), for 30 min at 25 °C, then P1 (8 μL, 10 μM), P2 (8 μL, 10 μM) and NMM (40 μL, 10 μM) were added. The mixtures were adjusted to 400 μL, incubated for one hour at 25 °C and measured by fluorescence. All fluorescence spectra of the samples were recorded on a Fluoromax-4 spectrofluorometer (Horiba Jobin Yvon Inc., France), utilizing slits of 5/5 nm, excitation at 399 nm, and emission at 608 nm.

2.3. UV melting and circular dichroism characterization

The melting profiles of nicked duplex I (PM/Ca/Cb), duplex II (PM/C) and G-quadruplex-duplex hybrid III (PM/P1/P2) were collected for the four groups of complementary DNAs. Relative absorbance at 260 nm was calculated based on formula of $(A_t–A_{10\ °C})/(A_{80}–A_{10\ °C})$. The melting temperature (T_m) was defined as the temperature when the relative absorbance was 0.5. The data of UV melting and circular dichroism (CD) was obtained on a JASCO J-820 spectropolarimeter (Tokyo, Japan). The absorbance was monitored at 260 nm as a function of temperature while ramping at a rate of 1 °C/min. The CD measurements were taken from 210 nm to 350 nm, the data pitch was 0.1 nm, scan speed was 200 nm/min, response time was 0.5 s, and bandwidth was 1 nm. 800 μL of each sample (Fig. 1A and Fig. S2) containing 1 μM of each indicated DNA and 50 mM KCl were prepared and annealed 4 °C overnight.

2.4. Fluorometric assays

The molar ratio of the PM, Ca and Cb was optimized as 1:1.5:1.5. 40 U/mL T4 and 20 U/mL *E. coli* DNA ligase in the 400 μL of final solutions were selected. For ATP detection, Ca (12 μL, 10 μM), Cb (12 μL, 10 μM), PM (8 μL, 10 μM), and 10 μL of T4 buffer were mixed with various concentrations of ATP. The mixtures were adjusted up to 78.4 μL with water, and incubated for 30 min at 37 °C. Then T4 DNA ligase (1.6 μL, 10 U/μL) was introduced into the mixtures to initiate the ligation reactions. After 1 h, KCl (20 μL, 1 M), P1 (8 μL, 10 μM), P2 (8 μL, 10 μM) and NMM (40 μL, 10 μM) were added, and then the solutions were adjusted up to 400 μL with Tris–HAc buffer. The samples were reacted for one hour at 25 °C and measured. For NAD^+ detection, samples were prepared using similar procedures for ATP, except for extra addition of 8 μL of BSA (0.05%) and utilization of E buffer (8 μL) and *E. coli* DNA ligase (1.6 μL, 5 U/μL) with different concentrations of cofactor NAD^+ instead of T4 buffer and T4 DNA ligase. The final concentrations of Ca, Cb, PM, KCl, P1, P2 and NMM were 300 nM, 300 nM, 200 nM, 50 mM, 200 nM, 200 nM and 1 μM, respectively. The differences of sample preparation for SNP analysis were that cofactor (ATP or NAD^+) was used at a fixed concentration of 20 μM, and single-base mismatches were employed as template DNA. To test the applicability of the strategy in biological fluid, 4 μL of human serum was introduced into the ligation solutions. After 1 h of ligation reaction, the mixtures containing 5% of human serum were heated at 95 °C for 5 min, cooled for one hour at 25 °C. After reaction with P1, P2, and NMM, the mixtures were centrifuged at 8000 rpm for 2 min to remove the denatured proteins. The supernatants were utilized for following fluorometric measurements.

2.5. Native polyacrylamide gel electrophoresis (native PAGE)

The ligation mixtures for PAGE analysis were prepared as follows: 4 μL of T4 or E buffer, Ca (6 μL, 10 μM), Cb (6 μL, 10 μM), 4 μL of template DNA (PM or its single mismatch, 10 μM), 8 μL of BSA (0.05%, only for *E. coli* DNA ligase) and cofactor (4 μL, 1 mM) were mixed together. The mixtures were adjusted up to 39.2 μL and incubated for 30 min at 37 °C. Then 0.8 μL of DNA ligase (10 U/μL T4 ligase or 5 U/μL *E. coli* DNA ligase) was added. After one hour of reaction at 37 °C, KCl (2 μL, 1 M), P1 (4 μL, 10 μM) and P2 (4 μL, 10 μM) were introduced. The final mixtures were incubated for one hour at 25 °C. Other samples containing indicated components were prepared using water as alternative component. The final concentrations of Ca, Cb, and template DNA, cofactor, P1, P2, and KCl were 1.2 μM, 1.2 μM, 0.8 μM, 80 μM, 0.8 μM, 0.8 μM, and 40 mM, respectively, and 0.16 U/μL T4 ligase and 0.08 U/μL *E. coli* DNA ligase in the 50 μL of final solutions were used. Polyacrylamide gels (10%, w/v) were prepared with 1 × TBE buffer (89 mM Tris, 89 mM boric acid, 2 mM EDTA and pH = 8.3). 10 μL of each sample was mixed with 1.5 μL of Gel-Dye, and loaded into the gel. The gels were run at 110 V for 40 min and photographed under UV light using a fluorescence imaging system (Vilber Lourmat, Marne laVallee, France).

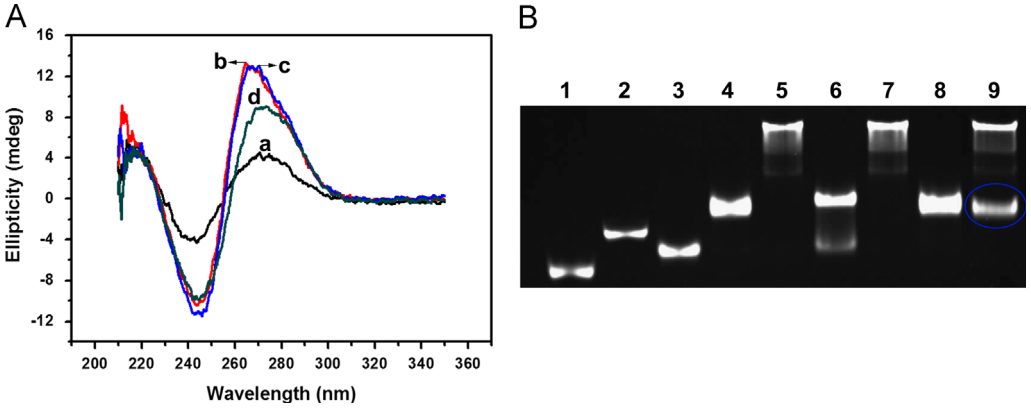

Fig. 1. (A) CD spectra of G-quadruplex from split G-quadruplex probes (P1/P2) with template PM in the presence of Ca2/Cb2 (c), or C2 (d). Curves a and b represent P1/P2 and PM/P1/P2, respectively. The concentration of each DNA strand was 1 μM, and 50 mM KCl was used in Tris-HAc buffer. (B) Native PAGE confirming DNA ligation by T4 DNA ligase and interaction between its products and split G-quadruplex probes. Lanes from 1 to 5 represent P1, P2, PM, PM/C2 and PM/P1/P2, respectively. Lanes 6 and 7 represent PM/Ca/Cb in the absence of T4 ligase without (6) or with (7) P1 and P2. Lanes 8 and 9 represent PM/Ca/Cb in the presence of T4 DNA ligase without (8) or with (9) P1 and P2. The band indicated by a blue circle is corresponding to ligation products. The final concentrations of PM, Ca, Cb, T4 DNA ligase, ATP, P1, P2, and KCl were 0.8 μM, 1.2 μM, 1.2 μM, 0.16 U/μL, 80 μM, 0.8 μM, 0.8 μM, and 40 mM, respectively in the diluted T4 buffer. (For interpretation of the references to color in this figure legend, the reader is referred to the web version of this article.)

3. Results and discussion

3.1. Strategy design and mechanism

T4 DNA ligase and *E. coli* DNA ligase were utilized to catalyze synthesis of phosphodiester bond between adjacent 5′-phosphoryl and 3′-hydroxyl groups in nicked duplex DNA (Lehnman, 1974). As shown in Scheme 1, the two short DNA probes (Ca and Cb) can be hybridized to the template PM, forming a nicked duplex (I). Then, DNA ligase joins the Ca and Cb into C and produces one repaired duplex (II). The split G-quadruplex probes (P1/P2) were obtained by splitting the c-Myc G-qudruplex DNA (TGAGGG TGGGGAG-GGTGGGGAA) (Phan et al., 2004) into two asymmetric fragments flanked with the sequences that were complementary to the template PM. In our previous report, it has been demonstrated that the template DNA can promote assembling of split G-quadruplex in the presence of potassium ion, the asymmetrically split G-quadruplex probes (P1/P2) used in this study have the highest sensitivity toward template DNA than the split probes of the other split modes, but cannot discriminate single-base mismatch well (Ren et al., 2012). The split G-quadruplex probes can displace PM from the nicked duplex I and reconstitute into the G-quadruplex-duplex hybrid structure (III), which binds NMM and emits intensive fluorescence. After DNA ligation, the G-quadruplex-duplex hybrid is not able to form, since the product duplex II is more stable than the hybrid III. Therefore, fluorescence decrease from G-quadruplex-NMM complex can be observed. As mentioned above, owing to the cofactor-dependent and mismatch-influenced ligation efficiency, the strategy was applied for cofactor detection and SNP discrimination.

The sequences of Ca and Cb were optimized using four groups of the partially complementary DNAs of PM (Table S1). Fig. S1 showed that the template PM in the presence of split G-quadruplex probes (P1/P2) caused fluorescence enhancement (column a and b), which was consistent with previous studies (Ren et al., 2012). Drastic fluorescence decrease was observed upon addition of DNAs from Ca2/Cb2 to C2 (column e and f). The data indicated that the two 9-mer DNAs (Ca2 and Cb2) were the optimal candidates for monitoring DNA ligation. Meanwhile, UV melting experiments were performed to interpret the underlying mechanism. According to the melting profiles shown in Fig. S2B, the melting temperature (T_m) values were obtained as 35 °C, 56 °C and 50 °C for nicked duplex I (PM/Ca2/Cb2), duplex II (PM/C2) and G-quadruplex-duplex hybrid III (PM/P1/P2), respectively. The relative thermodynamic stabilities (II > III > I) illustrated that the split G-quadruplex probes can acquire the template PM from the nicked duplex I to assemble into the G-quadruplex-duplex structure III, but cannot get it from duplex II. Through comparison of the T_m values of the structures (I, II and III) from the four groups of complementary sequences under the same condition (Fig. S2), it was concluded that the optimization of sequence length was very essential, because appropriate relative thermodynamic stabilities (ΔT_m) among the three structures (I, II and III) were critical for the sensitivity of the ligase-based systems.

The G-quadruplex was responsible for signal transduction in this strategy, so CD spectra were collected to demonstrate conformation changes of split G-quadruplex (Fig. 1A). The template PM-directed reassembling of G-quadruplex from split probes (P1/P2) was confirmed by an enhanced CD signal at 265 nm and 243 nm (curve a and b), which was consistent with the parallel structure of c-Myc G-quadruplex (Phan et al., 2004). Addition of Ca2 and Cb2 and formation of nicked duplex I did not influence the refolding of G-quadruplex of hybrid III according to the unchanged ellipticity (curve c). But the complementary DNA (C2) of PM decreased the ellipticity at 265 nm drastically (curve d), since duplex II inhibited the template-directed split G-quadruplex assembling. The CD results explicated the fluorescence decrease from G-quadruplex-NMM complex can be induced by DNA ligation of Ca and Cb.

3.2. DNA ligation coupled to split G-quadruplex probes

The Ca2 and 5′-phosphorated Cb2 were selected as Ca and Cb probes, respectively. The fluorescence quenching was observed with increasing amount of DNA ligase, suggesting that the DNA ligation reaction can be monitored by the coupling assay, and T4 and *E. coli* DNA ligase at final concentrations of 40 U/mL and 20 U/mL were selected for following experiments (Fig. S3). The concentrations of Ca and Cb were optimized using T4 DNA ligase (Fig. S4), and a molar ratio 1.5:1 for the probes (Ca/Cb) to the template PM was obtained and adopted in all ligation procedures.

Native PAGE was conducted to validate the products of DNA ligation and interaction between the products and split G-quadruplex probes. As revealed in lane 7 (Fig. 1B), the bright band corresponding to nicked duplex I (lane 6) disappeared in the presence of P1 and P2, and new bands produced corresponding to the G-quadruplex-duplex hybrid III (lane 5). After DNA ligation by T4 DNA ligase, a wide band corresponding to the mixture of duplex II (lane 4) and nicked duplex I can be observed in lane 8, as a result of the same 18 base pairs of I and II. When split G-quadruplex probes (P1/P2) were introduced into the ligation solution, two distinguishable bands were obtained in lane 9 and the one indicated by a blue circle was duplex II, since the nicked duplex I could not exist in the presence of P1 and P2 (lane 7). The similar PAGE data for *E. coli* DNA ligase was shown in Fig. S5. The PAGE results for T4 and *E. coli* DNA ligase illustrated that both DNA ligases can join the Ca and Cb together and generate the intact duplex II, and the split G-quadruplex probes were capable to distinguish the nicked duplex I from duplex II, which was because of the relative thermodynamic stabilities of the three DNA structures (II > III > I). Hence, it was well-founded that DNA ligation could inhibit the split probes to assemble into G-quadruplexes.

3.3. Cofactor detection

The non-covalent labeling strategy was utilized for cofactor detection based on the cofactor-dependent activity of DNA ligase. First, T4 DNA ligase was utilized to sensing ATP. As shown in Fig. 2A, intensive fluorescence was observed in the absence of ATP. Upon addition of ATP into the system, the ligation of the nicked duplex I was triggered, and the ligation products cannot supply the template PM for split G-quadrupelx probes (P1/P2), due to high thermodynamic stability of duplex II. Consequently, inhibition of G-quadruplex folding induced fluorescence quenching (Fig. 2A and B). A linear relationship was obtained between normalized fluorescence intensity (F_i) and the ATP concentration (C_{ATP}) from 50 nM to 0.6 μM (Inset in Fig. 2B), and the linear regression equation was $F_i = 1.0292 - 0.94902 \times C_{ATP}/\mu M$ ($R^2 = 0.997$). The 50 nM ATP corresponding to 2.7σ below the mean background level can be detected, and a limit of detection was calculated as 55 nM at a signal-to-noise (S/σ) of 3. The sensitivity is comparable and even superior to much previous ATP aptasensors (Sitaula et al., 2012; Song et al., 2012b; Wang et al., 2007). Titrations of NAD^+ were also conducted using *E. coli* DNA ligase. Similarly, fluorescence decreases were observed with increasing the NAD^+ (Fig. 2C and D), due to the NAD^+-dependent catalytic activity of *E. coli* DNA ligase. A calibration curve (Inset in Fig. 2D) showed a linear range between normalized fluorescence intensity (F_i) and NAD^+ concentration (C_{NAD}) from 10 nM to 200 nM and the regression equation was $F_i = 0.93544 - 0.0025 \times C_{NAD}/nM$ ($R^2 = 0.992$). The 10 nM NAD^+ ($S/\sigma = 2.1$) can be discriminated from the blank sample, and the defined detection limit ($S/\sigma = 3$) was calculated as 15 nM. In addition, as shown in Fig. 2, there was much more fluorescence quenching (70%) for NAD^+ than that (55%) for ATP and higher sensitivity for NAD^+ were obtained,

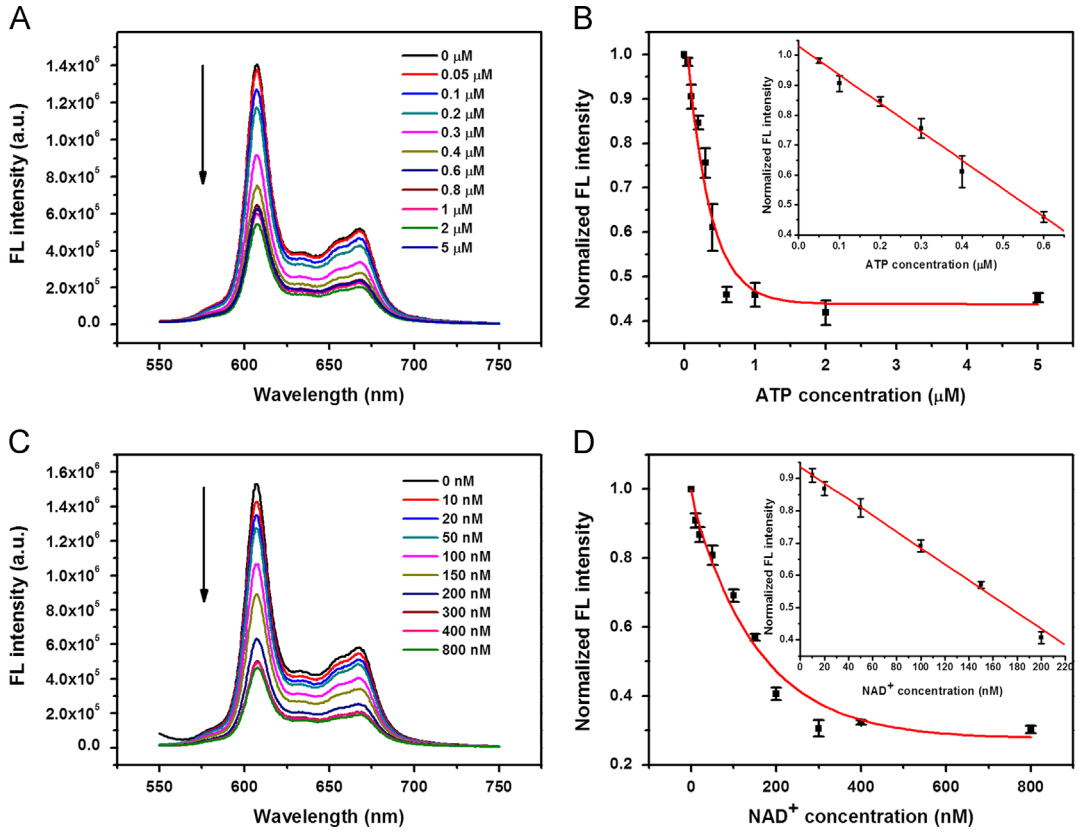

Fig. 2. Fluorescent spectra ((A) and (C)) and normalized fluorescence intensity at 608 nM ((B) and (D)) of the non-covalent labeling biosensor as function of concentration of ATP ((A) and (B)), or NAD^+ ((C) and (D)). The insets in graph (B) and (D) are the calibration curves for ATP and NAD^+, respectively. The final concentrations of PM, Ca, Cb, KCl, P1, P2 and NMM were 200 nM, 300 nM, 300 nM, 50 mM, 200 nM, 200 nM and 1 μM, respectively. The error bars indicate the standard deviation of three independent measurements for each concentration of target cofactor. T4 and *E. coli* DNA ligase at final concentrations of 40 U/mL and 20 U/mL were used for ATP and NAD^+ detection.

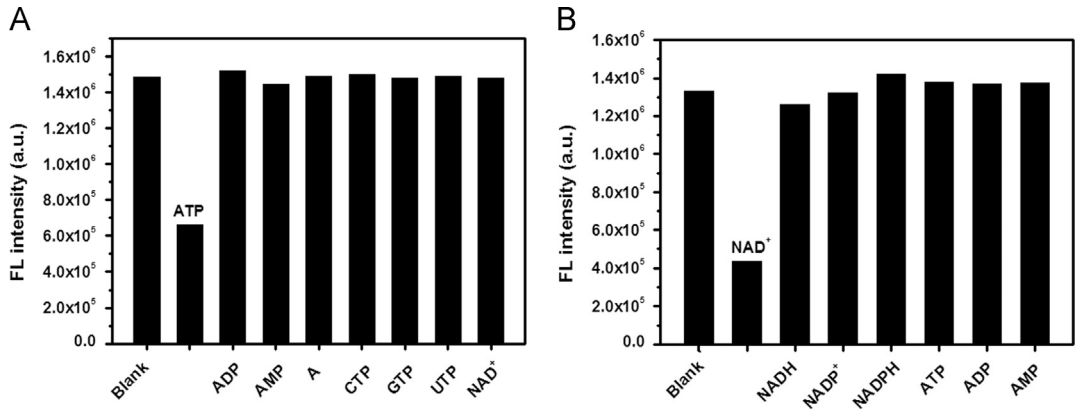

Fig. 3. Fluorescent responses of the ligase-based biosensor toward cofactor (ATP or NAD^+) and its analogues. The final concentrations of Ca, Cb, PM, KCl, P1, P2 and NMM were 300 nM, 300 nM, 200 nM, 50 mM, 200 nM, 200 nM and 1 μM, respectively. T4 and *E. coli* DNA ligase at final concentrations of 40 U/mL and 20 U/mL were used. The concentrations of cofactor and its analogues were all 1 μM.

which indicated that the NAD^+-dependent *E. coli* DNA ligase had much better ligation efficiency than ATP-dependent T4 ligase.

To evaluate the specificity of the strategy, we challenged our system with their analogues. Fig. 3A revealed that marked fluorescence decreases occurred only upon addition of ATP into system, and no obvious changes of fluorescence intensity were observed for the analogues including ADP, AMP, A, CTP, GTP, UTP and NAD^+. Most of previous G-quadruplex-based assays (He et al., 2012; Zhang et al., 2012) that used anti-ATP aptamer as recognition element, exhibited comparable sensitivity for ATP, but could not discriminate ATP from A, AMP and ADP. The data in Fig. 3B showed that addition of NAD^+ triggered drastic fluorescence quenching, while NADH, $NADP^+$, NADPH, ATP, ADP and AMP did not induce obvious fluorescence decrease. The excellent selectivity of our strategy for cofactor (ATP or NAD^+) was attributed to the high fidelity of the DNA ligase for cofactor, and made the sensing platform potential for analysis in complex samples.

3.4. SNP analysis

The aforementioned ligase-base assay also provides one simple and cost-effective strategy for transducing highly sequence-

dependent DNA ligation to readable fluorescent signal. Due to its better ligation efficiency, *E. coli* DNA ligase was employed for SNP discrimination. The effect of mismatch position of single-base mismatches on the ligation efficiency was investigated using this strategy. Sequences of single-base mismatches located at different positions from 5′ end of the PM sequence are shown in Table S2. It should be noted that PM and all the single-base mismatches can promote the formation of G-quadruplex-NMM complexes, which emitted intensive fluorescence (Fig. S6). As mentioned above, DNA ligation with perfectly matched template (PM) resulted in weak fluorescence. Conversely, enhanced fluorescence illustrated low ligation efficiency. As shown in Fig. 4A, ligation reactions were significantly hampered when the mismatch position was near the nick site (S17, S16 and S15), and the single-base mismatch at 3′ side exhibited much more intensive fluorescence than the one at 5′ side, indicating that the DNA ligase was much more sensitive to mutations at 3′ ligating end. The reason for a little signal enhancement for S12 was that lower stability of the duplex segment whose mutation was located near its center influenced ligase recognition and thus decreased the ligation efficiency. In excess of eight bases from the nick site (S24 and S8), the mismatch effect became unnoticeable. Meanwhile, the PAGE was performed to confirm the effect furthermore (Fig. 4B). The PAGE bands of ligation products that became distinguishable with the help of split probes (P1/P2) were indicated by a red rectangle. As anticipated, the PAGE results exactly coincided with fluorescence data. All the results illustrated that the effect of mismatch position on discrimination of single-base mismatch was validated by this strategy, which was in accordance with previous reports (Xue et al., 2009), and it was originated from directly and indirectly influence of ligase recognition at the nick site.

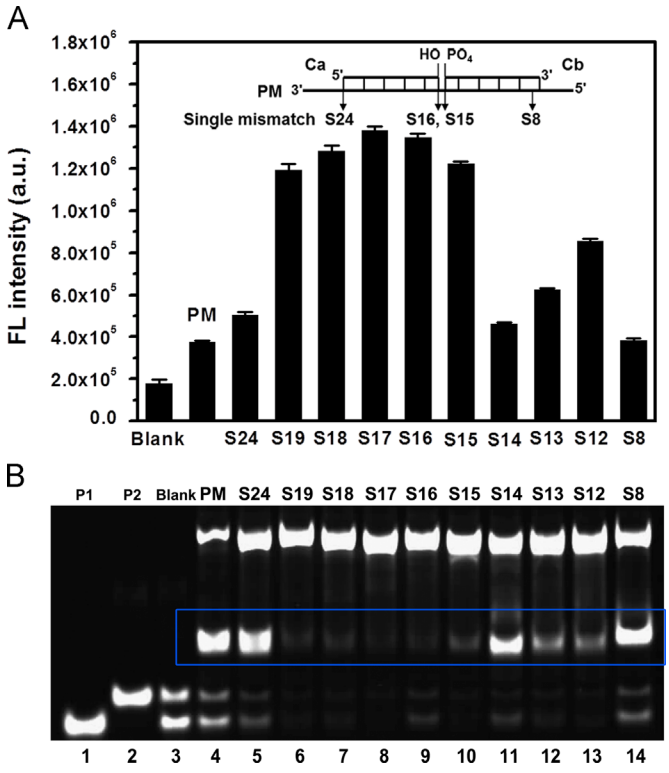

Fig. 4. (A) Fluorescent responses of the ligase-based system toward template DNA (PM or its single-base mismatches). The inset schematically shows the mismatch sites of PM. The final concentrations of Ca, Cb, template, NAD^+, *E. coli* DNA ligase, KCl, P1, P2 and NMM were 300 nM, 300 nM, 200 nM, 20 μM, 20 U/mL, 50 mM, 200 nM, 200 nM and 1 μM, respectively. The error bars were estimated from three independent measurements. (B) Native PAGE confirming the ligation products using PM and its single-base mismatches as template DNA (lane 4–14). Lanes 1 and 2 represent P1 and P2, respectively in the Tris–HAc buffer. The bands indicated by a blue rectangle are corresponding to ligation products. For samples (lane 4–14), the final concentrations of Ca, Cb, template, *E. coli* DNA ligase, NAD^+, P1, P2, and KCl were 1.2 μM, 1.2 μM, 0.8 μM, 0.08 U/μL, 80 μM, 0.8 μM, 0.8 μM, and 40 mM, respectively in the diluted E buffer. (For interpretation of the references to color in this figure legend, the reader is referred to the web version of this article.)

To furthermore confirm whether the strategy was applicable for SNP analysis, the T base of S16 was replaced with G and A. The data in Fig. 5A showed that fluorescence responses for all single-base mismatches of distinct mismatch types (G/T, G/A and G/G) were much higher than the signal for PM (G:C), and the maximum discrimination factor was 9.1 from G/A mismatch (the background was subtracted). As little as 1 nM single-base mismatch (S16) can be detected, while no obvious fluorescence change was observed when the PM concentration was below 25 nM (Fig. 5B). These results illuminated that SNP discrimination was realized by virtue of this simple protocol.

3.5. Strategy applicability in serum

Cofactor detection and SNP discrimination were performed in serum to investigate applicability of the non-covalent labeling strategy in biological fluid (Fig. S7, Table S3 and Fig. S8). The data exhibited that fluorescence backgrounds were increased greatly by addition of 5% serum into ligation solution as a result of interaction between fluorescent probes (NMM) and complex serum components, especially proteins. Thermal treatments were implemented after ligation reaction and before addition of split G-quadruplex probes and NMM, and the denatured proteins were

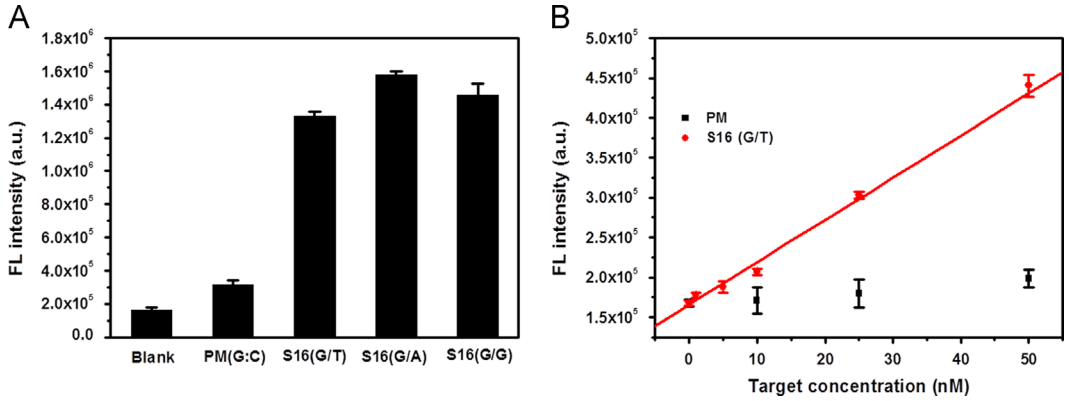

Fig. 5. (A) Fluorescent responses of the ligase-based system for SNP discrimination. The concentrations of PM and single-base mismatches were all 200 nM. (B) Fluorescent intensity at 608 nm as function of concentration of PM or S16 from 0 nM to 50 nM. The error bars estimated form three independent measurements. The final concentrations of Ca, Cb, NAD^+, *E. coli* DNA ligase, KCl, P1, P2 and NMM were 300 nM, 300 nM, 20 μM, 20 U/mL, 50 mM, 200 nM, 200 nM and 1 μM, respectively.

removed before measurement. Finally, the increased backgrounds were eliminated and sensitivities for cofactors and SNPs recovered absolutely. These results indicate that the DNA ligation reaction can proceed in complex biological fluids and the non-covalent labeling strategy is promising to be utilized for bioanalysis in practical and complex samples in future.

4. Conclusions

In summary, a versatile, non-covalent labeling and fluorescent strategy was fabricated for cofactor (ATP and NAD^+) detection and SNP discrimination based on inhibition of split G-quadruplex assembling by DNA ligation. Through tuning relative thermodynamic stabilities, DNA ligation was coupled to split G-quadruplex probes for the first time and fluorescence changes from non-covalent complex of G-quadruplex-fluorescent probe were recorded to monitor the ligation efficiency of DNA ligases. Due to cofactor-dependent ligation efficiency of DNA ligases (T4 and *E. coli* DNA ligase), specific detection of cofactor (ATP or NAD^+) was realized first. The detection limits in the nM range were obtained for ATP and NAD^+, respectively, and the sensing platform exhibited superior specificity toward cofactor as result of the high fidelity of DNA ligase for cofactor. Then, the effect of mismatch position of single-base mismatched template DNA on the ligation efficiency was validated. We demonstrated that the DNA ligase was much more sensitive to mutation at 3′ ligating end, but the mismatch effect was unnoticeable in excess of eight bases. Therefore, to acquire the best effect of SNP discrimination, it is necessary to change the captured probes (Ca and Cb) according to distinct mismatch positions of single-base mismatched target DNAs which can act as the template DNAs and promote G-quadruplex assembling. Because of its strong position-dependent response, this simple strategy has potential for identifying mismatched location of single-base mismatches of target DNA by a series of the coupling assays. SNP screening is anticipated to be realized by the simple fluorescent method in combination with signal amplification techniques. By virtue of thermal treatment, the strategy could function in serum, predicting its practical application in future. In addition, covalent modification of DNA probes with fluorescent probes was not required. The non-covalent labeling strategy provides a versatile and cost-effective platform for monitor of DNA ligation, cofactor detection, SNP analysis and other ligase-based assays.

Acknowledgements

This work was supported by the National Natural Science Foundation of China (No. 21190040, 11174105 and 91227114) and the 973 Project (2009CB930100) and the National Science Foundation.

Appendix A. Supporting information

Supplementary data associated with this article can be found in the online version at http://dx.doi.org/10.1016/j.bios.2013.07.059.

References

Burge, S., Parkinson, G.N., Hazel, P., Todd, A.K., Neidle, S., 2006. Nucleic Acids Research 34, 5402–5415.
Conze, T., Shetye, A., Tanaka, Y., Gu, J., Larsson, C., Göransson, J., Tavoosidana, G., Söderberg, O., Nilsson, M., Landegren, U., 2009. Annual Reviews of Analytical Chemistry 2, 215–239.
Gourine, A.V., Llaudet, E., Dale, N., Spyer, K.M., 2005. Nature 436, 108–111.
Guo, S., Du, Y., Yang, X., Dong, S., Wang, E., 2011. Analytical Chemistry 83, 8035–8040.
Harkness, R.A., Saugstad, O.D., 1997. Scandinavian Journal of Clinical and Laboratory Investigation 57, 655–672.
He, H.-Z., Pui-Yan, Ma, V., Leung, K.-H., Shiu-Hin Chan, D., Yang, H., Cheng, Z., Leung, C.-H., Ma, D.-L., 2012. Analyst 137, 1538–1540.
Hu, J., Zhang, C.-y., 2010. Analytical Chemistry 82, 8991–8997.
Jhaveri, S.D., Kirby, R., Conrad, R., Maglott, E.J., Bowser, M., Kennedy, R.T., Glick, G., Ellington, A.D., 2000. Journal of the American Chemical Society 122, 2469–2473.
Jia, H., Li, Z., Liu, C., Cheng, Y., 2010. Angewandte Chemie International Edition 49, 5498–5501.
Kolpashchikov, D.M., 2008. Journal of the American Chemical Society 130, 2934–2935.
Lehnman, I.R., 1974. Science 186, 790–797.
Li, T., Dong, S., Wang, E., 2010a. Journal of the American Chemical Society 132, 13156–13157.
Li, T., Shi, L., Wang, E., Dong, S., 2009. Chemistry—A European Journal 15, 1036–1042.
Li, T., Wang, E., Dong, S., 2010b. Analytical Chemistry 82, 1515–1520.
Lin, S.-J., Guarente, L., 2003. Current Opinion in Cell Biology 15, 241–246.
Liu, J.W., Cao, Z.H., Lu, Y., 2009. Chemical Reviews 109, 1948–1998.
Lowry, O.H., Passonneau, J.V., Schulz, D.W., Rock, M.K., 1961. Journal of Biological Chemistry 236, 2746–2755.
Lu, C.-H., Li, J., Lin, M.-H., Wang, Y.-W., Yang, H.-H., Chen, X., Chen, G.-N., 2010. Angewandte Chemie International Edition 49, 8454–8457.
Lu, L.-M., Zhang, X.-B., Kong, R.-M., Yang, B., Tan, W., 2011. Journal of the American Chemical Society 133, 11686–11691.
Ma, C., Yang, X., Wang, K., Tang, Z., Li, W., Tan, W., Lv, X., 2008. Analytical Biochemistry 372, 131–133.
Nakayama, S., Sintim, H.O., 2009. Journal of the American Chemical Society 131, 10320–10333.
Phan, A.T., Modi, Y.S., Patel, D.J., 2004. Journal of the American Chemical Society 126, 8710–8716.
Ren, J., Qin, H., Wang, J., Luedtke, N., Wang, E., Wang, J., 2011. Analytical and Bioanalytical Chemistry 399, 2763–2770.
Ren, J., Wang, J., Wang, J., Luedtke, N.W., Wang, E., 2012. Biosensors and Bioelectronics 31, 316–322.
Savas, S., Liu, G., 2009. Human Mutation 30, 1369–1377.
Sitaula, S., Branch, S.D., Ali, M.F., 2012. Chemical Communications 48, 9284–9286.
Song, J., Lv, F., Yang, G., Liu, L., Yang, Q., Wang, S., 2012a. Chemical Communications 48, 7465–7467.
Song, K., Kong, X., Liu, X., Zhang, Y., Zeng, Q., Tu, L., Shi, Z., Zhang, H., 2012b. Chemical Communications 48, 1156–1158.
Tang, Z., Liu, P., Ma, C., Yang, X., Wang, K., Tan, W., Lv, X., 2011. Analytical Chemistry 83, 2505–2510.
Tang, Z.W., Mallikaratchy, P., Yang, R.H., Kim, Y.M., Zhu, Z., Wang, H., Tan, W.H., 2008. Journal of the American Chemical Society 130, 11268–11269.
Wang, J., Wang, L., Liu, X., Liang, Z., Song, S., Li, W., Li, G., Fan, C., 2007. Advanced Materials 19, 3943–3946.
Wang, Y., He, X., Wang, K., Ni, X., 2010. Biosensors and Bioelectronics 25, 2101–2106.
Wee, E.J.H., Shiddiky, M.J.A., Brown, M.A., Trau, M., 2012. Chemical Communications 48, 12014–12016.
Xiao, X., Song, C., Zhang, C., Su, X., Zhao, M., 2012. Chemical Communications 48, 1964–1966.
Xu, Z., Singh, N.J., Lim, J., Pan, J., Kim, H.N., Park, S., Kim, K.S., Yoon, J., 2009. Journal of the American Chemical Society 131, 15528–15533.
Xue, X., Xu, W., Wang, F., Liu, X., 2009. Journal of the American Chemical Society 131, 11668–11669.
Yamada, K., Hara, N., Shibata, T., Osago, H., Tsuchiya, M., 2006. Analytical Biochemistry 352, 282–285.
Zhang, Z., Sharon, E., Freeman, R., Liu, X., Willner, I., 2012. Analytical Chemistry 84, 4789–4797.
Zhao, Y., Qi, L., Chen, F., Dong, Y., Kong, Y., Wu, Y., Fan, C., 2012. Chemical Communications 48, 3354–3356.
Zuo, X., Xia, F., Xiao, Y., Plaxco, K.W., 2010. Journal of the American Chemical Society 132, 1816–1818.
Zyryanov, G.V., Palacios, M.A., Anzenbacher, P., 2007. Angewandte Chemie International Edition 46, 7849–7852.